

# PCCP

Accepted Manuscript



This is an *Accepted Manuscript*, which has been through the Royal Society of Chemistry peer review process and has been accepted for publication.

*Accepted Manuscripts* are published online shortly after acceptance, before technical editing, formatting and proof reading. Using this free service, authors can make their results available to the community, in citable form, before we publish the edited article. We will replace this *Accepted Manuscript* with the edited and formatted *Advance Article* as soon as it is available.

You can find more information about *Accepted Manuscripts* in the [Information for Authors](#).

Please note that technical editing may introduce minor changes to the text and/or graphics, which may alter content. The journal's standard [Terms & Conditions](#) and the [Ethical guidelines](#) still apply. In no event shall the Royal Society of Chemistry be held responsible for any errors or omissions in this *Accepted Manuscript* or any consequences arising from the use of any information it contains.

## Fluorescence Switching of Sanguinarine in Micellar Environments

Sagar Satpathi, Krishna Gavvala, Partha Hazra \*

Department of Chemistry, Indian Institute of Science Education and Research (IISER)-Pune,  
Pune (411008), Maharashtra,  
India

---

\*Corresponding author E-mail: [p.hazra@iiserpune.ac.in](mailto:p.hazra@iiserpune.ac.in)

Tel.: +91-20-2590-8077; Fax: +91-20-2589 9790

## Abstract

Sanguinarine (SANG), a key member of benzyloquinoline alkaloids family, is well-known for its various therapeutic application such as antimicrobial, antitumor, anticancer, antifungal and anti-inflammatory etc. Depending on the medium pH, SANG exists in iminium or alkanolamine form, which emits at 580 nm and 420 nm, respectively. Nucleophilic attack on C<sub>6</sub> carbon atom converts the iminium form to alkanolamine form of SANG, and these two forms are equally important for the medicinal activities of SANG. To improve its potency as drug, it is essential to get a physical insight into this conversion process. In this study, we have deployed steady state and time-resolved spectroscopic techniques to probe this conversion process inside different micellar environments. We have observed that the conversion from iminium to alkanolamine form takes place in neutral OBG (octyl- $\beta$ -D-glucopyranoside glucose) and positively charged CTAB micelles, whereas iminium form exclusively exists in negatively charged SDS micelle. This conversion from iminium to alkanolamine form in case of OBG and CTAB micelles may be attributed to the reduced pK<sub>a</sub> of this conversion process owing to the enhanced hydrophobicity experienced by iminium form in between the surfactant head groups. On the other hand, the electrostatic attraction between positively charged iminium and negatively charged surfactant head groups stabilizes the iminium form in the stern layer of SDS micelle. We believe that our observations are useful for selective transportation of any particular form of the drug into the active site. Moreover, loading of any particular form of drug can be easily monitored with the help of fluorescence color switch from orange (iminium) to violet (alkanolamine) without pursuing any sophisticated or complex technique.

**Keywords:** Sanguinarine, iminium form, alkanolamine form, fluorescence color switch, time-resolved fluorescence.

## Introduction

From several years, naturally occurring alkaloids are receiving tremendous importance due to their potential pharmaceutical applications. Among them isoquinoline derivatives established itself as one of the foremost alkaloids owing to their important contribution in biomedical research.<sup>1</sup> Being a representative of benzyloisoquinoline alkaloids family,<sup>2, 3</sup> sanguinarine (SANG) exhibits numerous important biological activities such as anti-inflammatory, antioxidant, antifungal and antimicrobial etc.<sup>4-7</sup> Recent studies reveal that SANG can instigate apoptosis in various cancer cells.<sup>8</sup> Not only by inducing apoptosis, but also it can exhibit anticancer activity by means of inhibiting telomerase and topoisomerase enzyme activity.<sup>9, 10</sup> Thus, SANG can act as a G-quadruplex stabilizer and hence it prospects as a potential anticancer drug.<sup>10</sup> Due to its diverse application in biomedical research, some attention has been paid to understand the interactions of SANG with different biomolecules like protein, polymorphic nucleic acid structure including DNA (B form, Z form, triplex, G-quadruplex) and RNA etc.<sup>10-16</sup> SANG generally exist in two forms (Scheme 1) namely cationic form (i.e. iminium form) at lower pH ( $\leq 6.5$ ) and neutral form (i.e. alkanolamine form or pseudobase form) at higher pH ( $\geq 7.2$ ).<sup>17, 18</sup> The iminium form is unsaturated and completely planar; whereas alkanolamine form is non-planar one. The conversion from iminium to alkanolamine takes place due to nucleophilic attack of water/hydroxide ion on C<sub>6</sub> carbon atom, which is electrophilic in nature due to the presence of adjacent quaternary nitrogen atom.<sup>19</sup> The equilibrium between iminium and alkanolamine form is largely dependent on the pH of the medium.<sup>17</sup> Several biomolecules have different affinity for these two forms of SANG. Iminium form found to be the predominant form for binding with nucleic acid,<sup>16, 20</sup> whereas, exactly opposite binding

preference has been observed for interaction with serum protein i.e. alkanolamine form being the favored one.<sup>21</sup> The most unique property of SANG lies on its photophysical property due to its distinctly different emission maximum position for the iminium (580 nm) and alkanolamine form (420 nm).<sup>17</sup> The huge difference (~150 nm) in emission maximum between these two forms makes it very useful for probing the abasic site in DNA. Thus, SANG has been employed to find the abasic site in DNA. This shows that iminium form gets preference over the alkanolamine form in DNA abasic site, which is evident from their characteristics change in fluorescence peaks.<sup>22</sup> Likewise DNA abasic site, metalloprotein hemoglobin also found to have preference for iminium form.<sup>23</sup> Not only with biomolecules, SANG has also been studied in drug delivery vehicles like cucurbituril and cyclodextrin nano-cavities considering its potential usefulness in biomedical research. It was found that inside both the nano-cavities due to inhibition of nucleophilic attack iminium form is getting stabilized.<sup>18, 24</sup> In order to put forward SANG as a potential drug, it is very important to explore pharmacokinetic and pharmacodynamic behavior of the SANG, which will give a better insight about the characteristics properties of the drugs i.e. ADME (absorption, distribution, metabolism, and excretion). To monitor these characteristics, micelles are considered to be the simplest and useful model due to its eco-friendly nature and tunable properties.<sup>25, 26</sup>

Most of the biological systems in nature are highly anisotropic and restricted in nature. Inspired from nature, researchers have invested a reasonable amount of time in understanding the photophysical properties of drug inside biomimicking environments.<sup>27-31</sup> These biomimicking systems include self organized arrangements like micelle, reverse micelle, vesicles and molecular containers (i.e. cucurbituril, cyclodextrin etc.).<sup>18, 24, 31-33</sup> Among them, micelles are

considered to be one of the simplest ordered assemblies due to its highly cooperative, thermodynamically stable structure. Therefore, micelles have gained tremendous interest for its potential application in diverse fields as drug delivery vehicle, in energy storage and electronic devices.<sup>34-37</sup> Micelles have been widely utilized as drug carriers owing to their ability to enhance the solubility, stability and bio-availability of the drug by the incorporation of drug in micellar environments.<sup>25, 26</sup> Thus, it is necessary to understand the effect of micellar confinement on solubility and stability of SANG in order to use it in the pharmaceutical field. Moreover, to understand how SANG is transported to its target, it is very important to establish a relationship between the environment and the photophysical properties of SANG. In the present study, we have made an attempt to obtain the microenvironment alteration and photophysics modulation of SANG inside different types of micellar environment using steady state and time-resolved spectroscopy techniques. Interestingly, we have noticed that cationic and neutral micelles (i.e. CTAB and OBG) trigger the conversion from iminium to alkanolamine form, whereas iminium form is getting stabilization in anionic micelle (SDS). Moreover, our results suggest that this conversion from iminium to alkanolamine form can be easily monitored with the help of fluorescence switch from yellow to blue/violet color. We believe that our results might provide new insight towards the improvement of pharmaceutical applications of sanguinarine.

## Experimental Section

Sanguinarine (SANG), octyl- $\beta$ -D-glucopyranoside (OBG), sodium dodecyl sulfate (SDS), cetyltrimethylammonium bromide (CTAB) were purchased from Sigma Aldrich, and used without further purification. Millipore water (pH 6.5) was used for sample preparation. Surfactants were gradually added to the solution containing SANG, and the solution was gently shaken after each addition of surfactant until complete solubilization took place. Moreover, we have given 20 minutes equilibration time for each addition of surfactant. Buffer solution of pH 9 has been prepared using Tris-HCl salt.

Absorbance measurements were performed on Shimadzu UV-visible spectrophotometer (UV-2600), and steady-state fluorescence spectra were recorded in FluoroMax-4 spectrofluorimeter (Horiba Scientific, USA). All time-resolved fluorescence measurements (both life-time as well as anisotropy) were taken on a time correlated single photon counting (TCSPC) spectrometer (Horiba Jobin Yvon IBH, U.K.). The detail description of the instrument is described elsewhere.<sup>38,39</sup> Briefly, excitation of drug molecules have been done using 340 nm nano-led (pulse width  $\sim 1$  ns) and 375 nm (pulse width  $< 200$  ps) diode laser. For anisotropy ( $r(t)$ ) measurements, the emission polarization was adjusted to be parallel or perpendicular to that of the excitation, and anisotropy is defined as

$$r(t) = \frac{I_{\parallel}(t) - GI_{\perp}(t)}{I_{\parallel}(t) + 2GI_{\perp}(t)} \quad (1)$$

where  $I_{\parallel}(t)$  and  $I_{\perp}(t)$  are fluorescence decays polarized parallel and perpendicular to the polarization of the excitation light, respectively.  $G$  is the correction factor for detector sensitivity to the polarization direction of the emission and the measured  $G$  values are 0.5 and 0.62 for 340 nm and 375 nm excitation wavelength, respectively.  $G$  factor was measured using horizontally

polarization excitation light and collecting the horizontal ( $I_{HH}(t)$ ) and vertical ( $I_{HV}(t)$ ) decay profiles of emitted light. The analysis of lifetime and anisotropy data was done by IBH DAS6 analysis software. We have fitted both lifetime as well as anisotropy data with a minimum number of exponentials. Quality of each fitting was judged by  $\chi^2$  values and the visual inspection of the residuals. The value of  $\chi^2 \approx 1$  was considered as best fit for the plots. We have calculated the quantum yield of alkanolamine form and iminium form at pH 6.5 taking standard quantum yield value for alkanolamine and iminium form.<sup>22</sup>

## Results and Discussion

### Steady State Study:

Generally SANG exists in two form i.e. iminium and alkanolamine form (Scheme 1) and the conversion between these two forms is largely dependent on the pH of medium. The absorption spectrum of this iminium form offers four absorption bands in UV-vis range with peaks at 275, 330, 396 and 475 nm which corresponds to the electronic  $\pi \rightarrow \pi^*$  transition. But the same for alkanolamine exists only at 285 and 326 nm devoid of any band at higher wavelength.<sup>40</sup> In CTAB and OBG micelles, the characteristics peaks for iminium form (peaks at 396 and 475 nm) are getting reduced indicating the lesser ground state population of iminium form (Figure S1b and Figure S1c), whereas in SDS micelle it exhibits a small red shift (396 and 475 nm peak) suggesting the stabilization of iminium form of SANG (Figure S1a). Steady state emission studies have been performed to get insight into the excited state behavior of sanguinarine (SANG) in different type of micellar environments (Figure 1). Emission spectrum (excited at 320 nm) of SANG in water (pH  $\sim$  6.5) exhibits a dominating peak at 580 nm along with a peeping

peak at  $\sim 420$  nm (Figure 1). The lower energy peak is attributed to the iminium form of SANG, whereas the weak peak appeared at 420 nm indicates the presence of alkanolamine form of SANG.<sup>17, 18</sup> The presence of minute population of alkanolamine form is expected as the conversion from iminium to alkanolamine form takes place at  $\text{pH} \sim 7.5$ .<sup>17, 18</sup> With gradual addition of SDS to the SANG containing water solution, emission maximum at higher wavelength (at 580 nm) exhibits blue shift along with slight increment in intensity up to critical micelle concentration ( $< 8$  mM). After CMC ( $\geq 8$  mM), its characteristic peak of iminium form reappears at 580 nm and a small hike in intensity of alkanolamine peak at  $\sim 440$  nm (Figure 1a) is observed. The aberration in results below CMC ( $< 8$  mM) may be due to the electrostatic interaction between negatively charged SDS surfactant head group and positively charged drug molecule (Figure S2). Above CMC ( $\geq 8$  mM), the effect of micelle formation predominates over this electrostatic interaction; thereby, it shows enhancement and recovery of iminium form along with slight increment in alkanolamine peak intensity at  $\sim 450$  nm. Similar type of enhancement is also observed for excitation spectra monitored at 580 nm (i.e. iminium form) which indicates the stabilization of iminium form in SDS micellar environment (Figure S4). Noteworthy changes in fluorescence spectral features of SANG are observed in presence of CTAB (Figure 1b). On gradual increase in concentration of CTAB, the peak at  $\sim 420$  nm becomes prominent particularly after CMC. With further hike in concentration, the intensity at 420 nm tremendously increases along with blue shift; whereas the peak intensity at 580 nm systematically decreases, although it does not vanish even at very high concentration of CTAB (Figure 1b). Notably, at any concentration above CMC ( $> 8$  mM), the intensity of higher energy peak dominates over lower energy peak. Similar changes in emission spectral features are observed in case of OBG

micellar environment (Figure 1c). However, the peak at 420 nm is more blue shifted in OBG micellar environment compared to CTAB micelle (Figure 1c).

Notably, all the significant modulation in photophysical behavior of SANG comes into the picture above the respective CMC of surfactants. Thus, the changes in emission profiles observed are attributed to the effect of entrapment of SANG inside micellar environments. The most striking observation of our results is the prominent appearance of alkanolamine form of SANG in CTAB and OBG micelles. The observed increment in higher energy peak in both micellar systems (~420 nm) reflects the enhancement in alkanolamine population, and attenuation of lower energy peak (580 nm) indicates the gradual decrement in iminium form. In presence of CTAB and OBG micellar environment, excitation spectrum monitored at 580 nm (i.e. iminium form) decreases and the same for alkanolamine form (monitored at 420 nm) shows a gradual enhancement (Figure S5 and Figure S6). These observations lead us to conclude that the above two micellar environments favors the conversion from iminium to alkanolamine form of SANG. The tremendous increase in intensity of alkanolamine form compared to iminium form may be either due to the reduction of non-radiative decay pathway and/or increase in radiative decay pathway of the alkanolamine form of the SANG inside the micellar environment. Moreover, it is reported that the fluorescence quantum yield of alkanolamine form is significantly higher than the iminium form of SANG.<sup>17, 22</sup> The presence of iso-emissive point at 530 nm indicates that both the iminium and alkanolamine forms are in equilibrium in the excited state. The more blue shifted alkanolamine peak may be appearing due to the less polar environment experienced by SANG in presence of OBG micellar environment compared to CTAB micelle.

It is very well known that drug/probe molecule inside micelle can stay in three different locations, namely, Stern/palisade (ionic micelle/neutral micelle) layer, in between the surfactant head groups and hydrocarbon core of the micelle.<sup>41</sup> Stern/palisade layers are comprised of polar head group, counter ions (for ionic surfactants) and water molecules. Notably, the water molecules inside the Stern/palisade layer behave differently compared to bulk water.<sup>42</sup> Even the dynamics of these water molecules in micellar environments are drastically retarded compared to bulk water medium.<sup>41</sup> Positively charged SANG molecules (i.e. its iminium form) prefer to stay in the negatively charged Stern layer of SDS micelles due to the electrostatic interaction, which leads to the stabilization of this cationic form of the drug. In consequence, the emission peak at lower energy (580 nm) is getting enhanced with the gradual addition of SDS surfactant. Unlike SDS, the Stern layer of CTAB micelle is positively charged, whereas the palisade layer of OBG micelle is neutral. Thus, the positively charged SANG (i.e. iminium form) molecules do not experience any stabilization in the Stern/palisade layer of these micelles (CTAB and OBG). Hence, the drug molecules try to stay away from the Stern /palisade layer and preferably reside in between the surfactant head groups. Here, it is pertinent to mention that  $pK_a$  of the probe is getting modulated by the hydrophobicity of the medium.<sup>43,44</sup> A greater hydrophobicity in micellar environment can decrease the  $pK_a$  of the probe due to less polarity of the surrounding environment.<sup>43-45</sup> Positively charged SANG (iminium form) molecules in between the surfactant head groups experience a reasonable amount of hydrophobicity than that of in bulk water medium. This makes the C6 carbon (adjacent to positively charged nitrogen atom) atom to be more electron deficient in nature. Thus, the conversion from iminium to alkanolamine form becomes even more facile in these micellar environments (CTAB, OBG). Notably, it is reported

that pH of water molecules residing at the CTAB micellar surface is higher ( $\text{pH} \sim 9.5$ ) than that of bulk water ( $\text{pH} = 7$ ).<sup>44, 45</sup> This may be another contributing factor for this conversion process in CTAB micellar environment.<sup>45</sup> Based on these facts, it is logical to predict that  $\text{pK}_a$  for the conversion between iminium to alkanolamine form decreases in presence of OBG and CTAB micellar environments. We have also calculated the percentage of molecule being converted from iminium to alkanolamine form by monitoring the reduction in emission intensity at 580 nm exciting iminium form exclusively at 475 nm (Figure S3). Our calculation suggests that percentage of molecules converted from iminium to alkanolamine form are  $\sim 50\%$  and  $\sim 60\%$  for OBG and CTAB micelles, respectively. In a nutshell, the steady state results of SANG in presence of micellar environments manifest the fact that the conversion from iminium to alkanolamine form can be probed in CTAB and OBG micelles, without increasing pH of the medium.

#### **Time Resolved Study:**

We have employed time-resolved fluorescence measurement technique, which is an excellent tool to monitor the dynamics of molecules in the excited state, and is a sensitive technique in identifying multiple emissive species present in a system. Decay profiles of SANG in the absence and presence of micellar environments are collected at  $\sim 400$  nm (exciting by 340 nm nano-led) and 580 nm (exciting at 375 nm diode laser) to monitor the excited-state dynamics of alkanolamine and iminium forms, respectively. Fluorescence transients are shown in Figure 2 and the results are presented in Table 1. Iminium and alkanolamine forms in water exhibit a single exponential decay (collected at 580 nm and 415 nm, respectively) with lifetime of 2.37 ns

and 3.16 ns, respectively. In case of SDS micelle, the lifetime of iminium form increases from 2.37 (in water) to 4.82 ns (Table 1). This observation confirms our claim that positively charged iminium form residing at the Stern layer of SDS micelle gets stabilization through electrostatic interaction with the negatively charged head group of the surfactant. This confinement of the iminium form inside the micellar environment reduces the non-radiative decay pathways to several fold, which accounts for the increment in excited state lifetime. In case of OBG micellar environment, the lifetime of alkanolamine form (monitored at 420 nm) increases, whereas the decrement in lifetime is observed in CTAB micelle (Table 1). The increased lifetime in OBG micelle may be attributed to the encapsulation of the drug in confined environment. Moreover, the lifetime of alkanolamine form reduces in CTAB micelle. The above mentioned lifetime results can be rationalized in terms of alternations in radiative and non-radiative decay pathways (eqn. 2 and 3) of SANG in presence of confined micellar environments.

$$\phi_f = k_r \tau_f \quad (2)$$

$$\frac{1}{\tau_f} = k_r + \sum k_{nr} \quad (3)$$

Where  $\phi_f$  represents quantum yield,  $\tau_f$  is lifetime of the excited state species.  $k_r$  and  $k_{nr}$  are the radiative and non-radiative rate constants, respectively. We have calculated quantum yields, radiative and non-radiative constants for respective systems which are listed in Table 2. Since the ~~average~~ lifetime of the alkanolamine form is reduced (Table 1) and the intensity of the same form is enhanced in the presence of CTAB micellar environment (Figure 2b), it suggests the increase in the radiative rate constant ( $k_r$ ) of alkanolamine form (0.41 ps<sup>-1</sup> to 31 ps<sup>-1</sup>) is significantly higher than the change in the non-radiative decay rate constant ( $k_{nr}$ ) of

alkanolamine form. In fact the non-radiative decay rate constant ( $k_{nr}$ ) of alkanolamine form enhances in presence of CTAB micellar environment ( $309 \text{ ps}^{-1}$  to  $320 \text{ ps}^{-1}$ ). But in case of OBG micellar environment, non-radiative ( $k_{nr}$ ) and radiative decay constant ( $k_r$ ) of alkanolamine form is found to be decreased and increased, respectively, which is also evident from their respective changes in quantum yield and excited state lifetime value (Table 2). This increment in non-radiative decay channels in CTAB micelles can be rationalized in terms of heavy atom perturbation effect.<sup>46</sup> The presence of bromide ions promote the intersystem crossing phenomenon ( $S_1 \rightarrow T_1$ ) via spin-orbit coupling.<sup>47</sup> Thus, the excited state lifetime of alkanolamine form decreases in presence of CTAB micellar environment due to the enhancement in non-radiative decay pathways. Similar kinds of enhancement in non-radiative decay pathways are also perceived for many organic compounds in CTAB micellar environment.<sup>48,49</sup> The same effect is absent in OBG micelles, as the micellar surface is devoid of any heavy ions. Therefore, its lifetime increases due to the confinement effect in OBG micellar environment. In summary, the lifetime results are in harmony with the steady state results, which infers that the conversion from iminium to alkanolamine takes place inside OBG and CTAB micelles, whereas iminium form gets stabilization in SDS micelle.

Time-resolved anisotropy measurement has been employed to get an idea about the location as well as surrounding environments around the drug. The rotational relaxation time of SANG in water (pH 6.5) occurs on a  $\sim 160 \text{ ps}$  timescale (monitored at emission maxima of iminium form at  $580 \text{ nm}$  by exciting at  $375 \text{ nm}$ ). Anisotropy decay transients for SANG in different micellar environment shows significant change in rotational relaxation time (Table 3, Figure 3). In case of OBG and CTAB micellar systems, anisotropy decay profiles show the

increment in average rotational relaxation time to nanosecond time scale (1.97 ns for CTAB and 2.30 ns for OBG micelle). This increase in rotational relaxation time is indicative for the confinement for SANG molecule inside CTAB and OBG micelles. In case of SDS micelle, the anisotropy transient (monitored at 580 nm) fitting exhibits a rotational relaxation time of ~750 ps, which is almost five times slower in comparison with the rotational relaxation time of SANG in water. More retarded rotational relaxation time in CTAB and OBG micelles than that of SDS micelle suggests that drug molecules located in more restricted environment in former two micelles, probably resides in between surfactant head groups; whereas in SDS micelle, drug molecules stays at the Stern layer exhibiting faster relaxation dynamics (~ 0.7 ns) compared to other micellar environments. We have also determined the hydrodynamic diameter of the drug-micelle complex from the Stokes–Einstein relationship<sup>50</sup> (Note S1). The obtained hydrodynamic diameter values for different micelles (Table 3) are in good agreement with literature values,<sup>51-53</sup> which further validate the encapsulation of the drug in micellar environment. In summary, anisotropy results confirm that positively charged SANG molecules reside at the negatively charged Stern layer of SDS micelle and gets stabilization in this micellar environment, whereas SANG molecules encapsulated in between polar head groups (with pyridine nitrogen exposing towards the surface) experience reasonable amount of hydrophobicity in OBG and CTAB micelles, and is majorly responsible for the change in  $pK_a$  of drug molecules and subsequent conversion from iminium to alkanolamine form of SANG.

SANG exhibits different binding mode with several supramolecular assemblies and biological nano-cavities.<sup>18, 21, 23, 24</sup> In biological nano-cavity (like serum protein, hemoglobin), preference for both the iminium and alkanolamine forms have been observed. Serum protein

found to have more binding affinity for alkanolamine form,<sup>21</sup> whereas the exactly opposite binding preference has been observed for hemoglobin.<sup>23</sup> Binding of positively charged iminium form is majorly driven through the electrostatic interaction with amino acid residue, whereas hydrophobicity plays the key role for alkanolamine form.<sup>21, 23</sup> Bicz'ok and co-workers reported the the preferential encapsulation of the iminium form and the protection of the C6 position of sanguinarine against the nucleophilic attack by hydroxide anion.<sup>18</sup> Similar kind of binding affinity (iminium form encapsulation) has been also observed in cyclodextrin nano-cavity and this binding is found to be entropy driven due to the release of water molecule from cyclodextrin cavity.<sup>24</sup> In contrast with previously reported literatures, our work shows that different forms (iminium and alkanolamine) of SANG can be stabilized in different micellar environments. However, this feature is found to be absent in other drug delivery vehicles, like, cyclodextrin and cucurbituril, which have selective preference for iminium form over alkanolamine form.<sup>18, 24</sup> Moreover, loading of this drug can be easily monitored with the help of fluorescence switch from orange (iminium) to violet (alkanolamine) without pursuing any sophisticate or complex technique, which may have significant application in the selective transportation of the drug in its active sites. As biomolecules have different affinity towards these two active forms of SANG (iminium and alkanolamine), we believe that our results may provide some new insight into the transportation of particular form of SANG to its target site using micelle as a drug delivery vehicle.

## Conclusion

In this article, we have attempted to endeavor the physiochemical modulation of a potential anticancer drug, sanguinarine (SANG) inside different surface charged micellar arrangements. In CTAB (positively charged) and OBG (neutral) micelles, conversion from iminium to alkanolamine form is confirmed from their respective changes in absorption and fluorescence spectra. Emission maximum at 580 nm (for iminium form) is shifted to characteristics alkanolamine peak at 420 nm in the above mentioned two micellar environments, and this conversion process is attributed to decreased  $pK_a$  of SANG molecule inside these micelles. However, in case of negatively charged SDS micelle, iminium form is getting stabilization at the stern layer of micelle due to electrostatic attraction between positively charged iminium and negatively charged surfactant head groups. Time-resolved lifetime and anisotropy studies also upheld these facts and nicely compliments with our steady state results in different micelles. Keeping the enormous biological applications of SANG in mind, our photophysical studies of SANG in bio-mimicking organized assemblies (i.e. micelles) may be helpful towards understanding its potential therapeutic applications.

## Acknowledgements

Authors thank IISER-Pune for providing excellent experimental facilities. The authors are thankful to anonymous reviewers for their valuable comments and suggestions.

## References

1. V. M. Dembitsky, T. A. Gloriovova and V. V. Poroikov, *Phytomedicine*, 2015, 22, 183-202.
2. M. Reina and A. González-Coloma, *Phytochem. Rev.*, 2007, 6, 81-95.
3. G. B. Mahady and C. W. W. Beecher, *Planta Med*, 1994, 60, 553-557.
4. N. Ahmad, S. Gupta, M. M. Husain, K. M. Heiskanen and H. Mukhtar, *Clin. Cancer Res.*, 2000, 6, 1524-1528.
5. I. D. Mandel, *J. Am. Dent. Assoc.*, 1994, 125, 2S-10S.
6. I. De Stefano, G. Raspaglio, G. F. Zannoni, D. Travaglia, M. G. Prisco, M. Mosca, C. Ferlini, G. Scambia and D. Gallo, *Biochem. Pharmacol.*, 2009, 78, 1374-1381.
7. V. M. Adhami, M. H. Aziz, S. R. Reagan-Shaw, M. Nihal, H. Mukhtar and N. Ahmad, *Mol. Cancer Ther.*, 2004, 3, 933-940.
8. A. R. Hussain, N. A. Al-Jomah, A. K. Siraj, P. Manogaran, K. Al-Hussein, J. Abubaker, L. C. Platanias, K. S. Al-Kuraya and S. Uddin, *Cancer Res.*, 2007, 67, 3888-3897.
9. J. Holy, G. Lamont and E. Perkins, *BMC Cell Biol.*, 2006, 7, 1-12.
10. I. Bessi, C. Bazzicalupi, C. Richter, H. R. A. Jonker, K. Saxena, C. Sissi, M. Chioccioli, S. Bianco, A. R. Bilia, H. Schwalbe and P. Gratteri, *ACS Chem. Biol.*, 2012, 7, 1109-1119.
11. P. Giri and G. S. Kumar, *BBA-Gen. Subjects*, 2007, 1770, 1419-1426.
12. A. Adhikari, M. Hossain, M. Maiti and G. Suresh Kumar, *J. Mol. Struct.*, 2008, 889, 54-63.
13. L.-P. Bai, Z. Cai, Z.-Z. Zhao, K. Nakatani and Z.-H. Jiang, *Anal. Bioanal. Chem.*, 2008, 392, 709-716.
14. J. Urbanová, P. Lubal, I. Slaninová, E. Tábořská and P. Tábořský, *Anal. Bioanal. Chem.*, 2009, 394, 997-1002.
15. M. Hossain, A. Y. Khan and G. Suresh Kumar, *PLoS ONE*, 2011, 6, e18333.
16. M. Hossain, A. Kabir and G. Suresh Kumar, *J. Biomol. Struct. Dyn.*, 2012, 30, 223-234.
17. M. Maiti, R. Nandi and K. Chaudhuri, *Photochem. Photobiol.*, 1983, 38, 245-249.
18. Z. Miskolczy, M. Megyesi, G. Tarkanyi, R. Mizsei and L. Biczok, *Org. Biomol. Chem.*, 2011, 9, 1061-1070.
19. J. í. Dostál and M. Potá?ek, *Collect. Czech. Chem. C.*, 1990, 55, 2840-2873.
20. A. Sen and M. Maiti, *Biochem. Pharmacol.*, 1994, 48, 2097-2102.
21. M. Hossain, A. Y. Khan and G. Suresh Kumar, *J. Chem. Thermodyn.*, 2012, 47, 90-99.
22. F. Wu, Y. Sun, Y. Shao, S. Xu, G. Liu, J. Peng and L. Liu, *PLoS ONE*, 2012, 7, e48251.
23. S. Hazra and G. Suresh Kumar, *J. Phys. Chem. B*, 2014, 118, 3771-3784.
24. S. Hazra and G. S. Kumar, *RSC Adv.*, 2015, 5, 1873-1882.
25. K. Kataoka, A. Harada and Y. Nagasaki, *Adv. Drug Deliver. Rev.*, 2001, 47, 113-131.
26. M. L. Turco Liveri, M. Licciardi, L. Sciascia, G. Giammona and G. Cavallaro, *J. Phys. Chem. B*, 2012, 116, 5037-5046.
27. N. J. Turro, J. K. Barton and D. A. Tomalia, *Accounts Chem. Res.*, 1991, 24, 332-340.
28. R. Chakrabarty, P. S. Mukherjee and P. J. Stang, *Chem. Rev.*, 2011, 111, 6810-6918.
29. R. Villalonga, R. Cao and A. Frago, *Chem. Rev.*, 2007, 107, 3088-3116.
30. C. Ghatak, V. G. Rao, S. Mandal, S. Ghosh and N. Sarkar, *J. Phys. Chem. B*, 2012, 116, 3369-3379.
31. S. Mandal, V. G. Rao, C. Ghatak, R. Pramanik, S. Sarkar and N. Sarkar, *J. Phys. Chem. B*, 2011, 115, 12108-12119.
32. H. C. Junqueira, D. Severino, L. G. Dias, M. S. Gugliotti and M. S. Baptista, *Phys. Chem. Chem. Phys.*, 2002, 4, 2320-2328.
33. B. Bangar Raju and S. M. B. Costa, *Phys. Chem. Chem. Phys.*, 1999, 1, 5029-5034.

34. B. Maity, A. Chatterjee, S. A. Ahmed and D. Seth, *J. Phys. Chem. B*, 2015, 119, 3776-3785.
35. C. C. Bof Bufon, J. D. Cojal González, D. J. Thurmer, D. Grimm, M. Bauer and O. G. Schmidt, *Nano Lett.*, 2010, 10, 2506-2510.
36. M. Boncheva, D. H. Gracias, H. O. Jacobs and G. M. Whitesides, *Proceedings of the National Academy of Sciences*, 2002, 99, 4937-4940.
37. K. M. Gangotri, R. C. Meena and R. Meena, *J. Photoch. Photobio. A*, 1999, 123, 93-97.
38. A. Sengupta, R. V. Khade and P. Hazra, *J. Phys. Chem. A*, 2011, 115, 10398-10407.
39. K. Gavvala, W. D. Sasikala, A. Sengupta, S. A. Dalvi, A. Mukherjee and P. Hazra, *Phys. Chem. Chem. Phys.*, 2013, 15, 330-340.
40. I. G. Motevich, N. D. Strekal, J. W. Nowicky and S. A. Maskevich, *J. Appl. Spectrosc.*, 2010, 77, 394-399.
41. N. Sarkar, K. Das, A. Datta, S. Das and K. Bhattacharyya, *J. Phys. Chem.*, 1996, 100, 10523-10527.
42. N. Nandi, K. Bhattacharyya and B. Bagchi, *Chem. Rev.*, 2000, 100, 2013-2046.
43. V. E. Yushmanov, J. R. Perussi, H. Imasato, A. C. Ruggiero and M. Tabak, *Biophys. Chem.*, 1994, 52, 157-163.
44. M. S. Fernandez and P. Fromherz, *J. Phys. Chem.*, 1977, 81, 1755-1761.
45. D. Roy, R. Karmakar, S. K. Mondal, K. Sahu and K. Bhattacharyya, *Chem. Phys. Lett.*, 2004, 399, 147-151.
46. J. C. Koziar and D. O. Cowan, *Accounts Chem. Res.*, 1978, 11, 334-341.
47. S. P. McGlynn, M. J. Reynolds, G. W. Daigre and N. D. Christodouleas, *J. Phys. Chem.*, 1962, 66, 2499-2505.
48. T. Wolff, *Berichte der Bunsengesellschaft für physikalische Chemie*, 1982, 86, 1132-1134.
49. V. Ramesh and V. Ramamurthy, *Journal of Photochemistry*, 1984, 24, 395-402.
50. J. R. Lakowicz, *Principles of Fluorescence Spectroscopy*, Springer, New York, 3rd edn., 2006.
51. G. Duplâtre, M. F. Ferreira Marques and M. da Graça Miguel, *J. Phys. Chem.*, 1996, 100, 16608-16612.
52. B. K. Paul, D. Ray and N. Guchhait, *J. Phys. Chem. B*, 2012, 116, 9704-9717.
53. B. Lorber, J. B. Bishop and L. J. DeLucas, *Biochimica et Biophysica Acta (BBA) - Biomembranes*, 1990, 1023, 254-265.

**Table 1.** Fluorescence transient fittings of sanguinarine in water, buffer and different micellar environments.

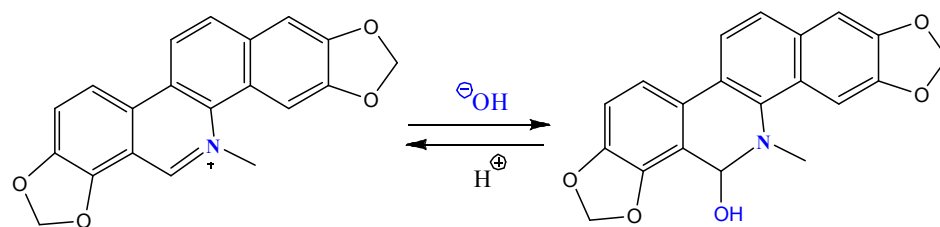
Sample	$\lambda_{\text{ex}}$ (nm)	$\lambda_{\text{em}}$ (nm)	$a_1$	$\tau_1$ (ns)	$\chi^2$
SANG in water (pH 6.5)	375	580	1	2.38	0.99
SANG + 41 mM SDS	375	580	1	4.82	1.09
SANG + 163 mM OBG	375	580	1	3.08	1.16
SANG + 32.5 mM CTAB	375	580	1	2.28	1.05
SANG in buffer (pH 9.5)	340	415	1	3.16	1.04
SANG + 163 mM OBG	340	403	1	3.85	1.04
SANG + 32.5 mM CTAB	340	415	1	2.88	1.05

**Table 2.** Quantum yields, radiative and non-radiative constants of sanguinarine in water (pH 6.2) and different micellar environments.

Sample	$\phi_f$	$\tau_{\text{avg}}$ (ns)	$k_r \times 10^{12} (\text{s}^{-1})$	$k_{\text{nr}} \times 10^{12} (\text{s}^{-1})$
SANG in H <sub>2</sub> O (iminium) pH 6.5	0.00307	2.38	1.29	419
SANG in SDS (iminium)	0.00594	4.82	1.23	206
SANG in buffer (alkanolamine) pH 9.5	0.0013	3.16	0.41	309
SANG in OBG (alkanolamine)	0.0683	3.85	17.7	240
SANG in CTAB (alkanolamine)	0.09	2.88	31	320

**Table 3.** Time-resolved anisotropy decay parameters of sanguinarine in water, buffer and different micellar environments.

Sample	$\lambda_{\text{ex}}$ (nm)	$\lambda_{\text{em}}$ (nm)	$\tau_1$ (ns)	$a_1$	$\tau_2$ (ns)	$a_2$	$\tau_r$ <ns>	$D_h$ (Å)	$\chi^2$
SANG in water pH 6.5	375	580	0.16	1	-	-	0.16	-	1.02
SANG + 41 mM SDS	375	580	0.75	1	-	-	0.75	18.06	1.04
SANG + 163 mM OBG	340	404	0.36	0.10	2.50	0.90	2.30	26.24	1.04
SANG + 32.5 mM CTAB	340	415	0.36	0.06	2.07	0.94	1.97	24.92	1.05
SANG in pH 9.5 Buffer	340	420	0.35	1	-	-	0.35	-	0.94



**Scheme 1.** Chemical structures of iminium and alkanolamine form of sanguinarine.

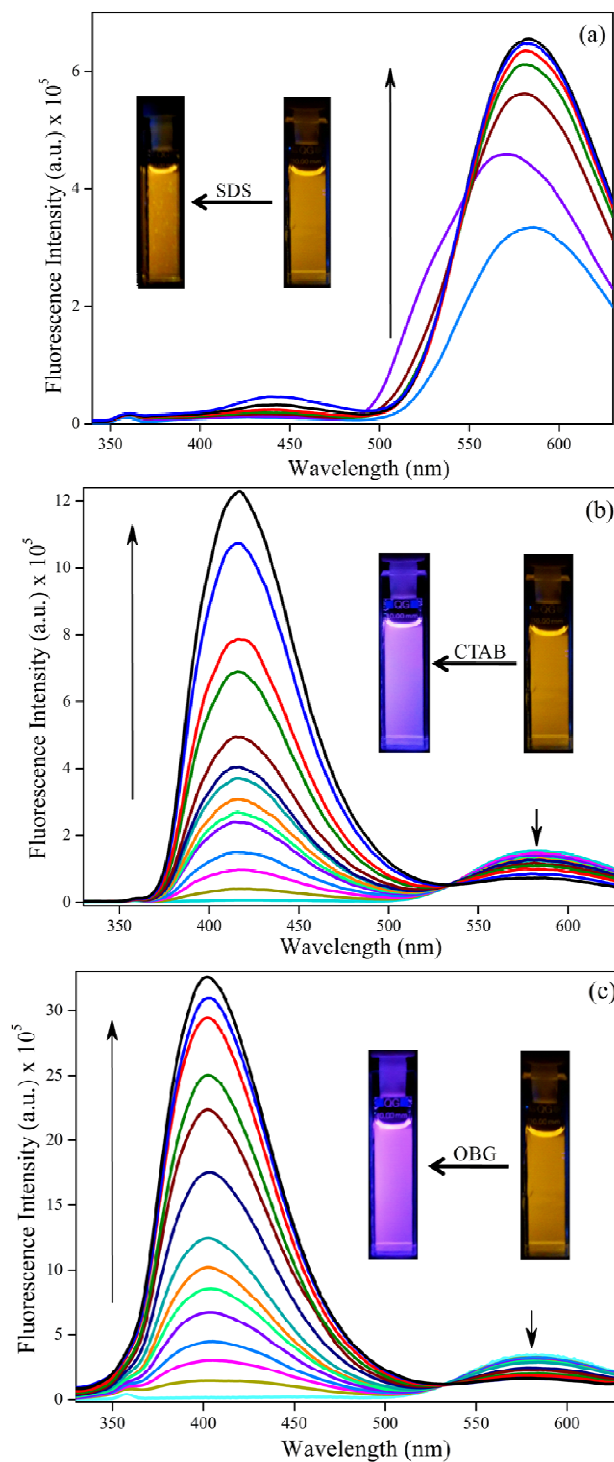


**Figure 1.** Emission spectra of sanguinarine (~10 μM) with increasing concentration of different types of surfactants (a) SDS (0 to 41 mM), (b) CTAB (0 to 32.5 mM) and (c) OBG (0 to 163 mM). The direction of arrow indicates lower to higher concentration.

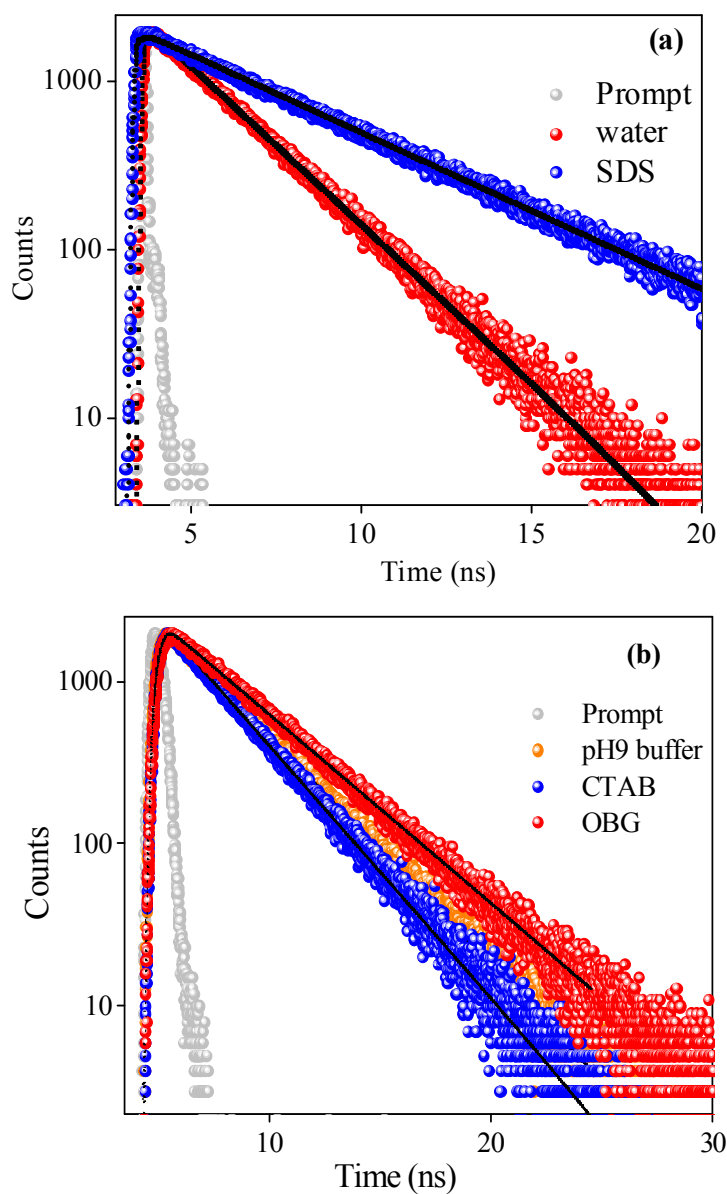


**Figure 2.** Fluorescence transients of sanguinarine (a) in water and SDS ( $\lambda_{\text{ex}} = 375$  nm,  $\lambda_{\text{em}} = 580$  nm), (b) in pH 9 buffer ( $\lambda_{\text{ex}} = 340$  nm,  $\lambda_{\text{em}} = 420$  nm), CTAB ( $\lambda_{\text{ex}} = 340$  nm,  $\lambda_{\text{em}} = 415$  nm) and OBG ( $\lambda_{\text{ex}} = 340$  nm,  $\lambda_{\text{em}} = 403$  nm) micelles.

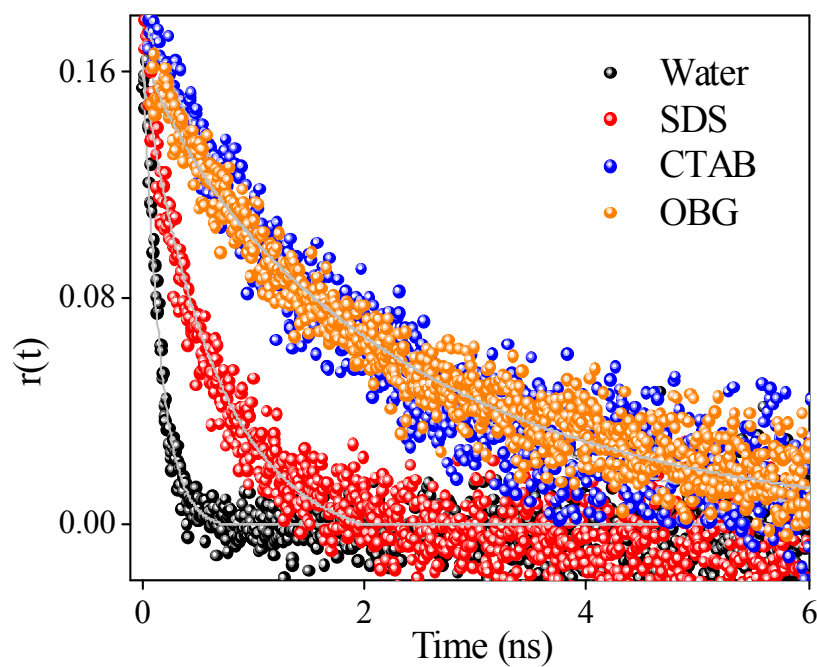


**Figure 3.** Anisotropy decays of sanguinarine in water ( $\lambda_{\text{ex}}=375$  nm,  $\lambda_{\text{em}}=580$  nm), CTAB ( $\lambda_{\text{ex}}=340$  nm,  $\lambda_{\text{em}}=415$  nm), OBG ( $\lambda_{\text{ex}}=340$  nm,  $\lambda_{\text{em}}=404$  nm) and SDS ( $\lambda_{\text{ex}}=375$  nm,  $\lambda_{\text{em}}=580$  nm) micelles.

“Table of Contents”

